Acta Cryst. (1975). B31, 1666

Mo_5O_{14} – Twinning and Three-Dimensional Structure, Determined from a Partly Tantalum-Substituted Crystal

BY NOBORU YAMAZOE* AND LARS KIHLBORG

Department of Inorganic Chemistry, Arrhenius Laboratory, University of Stockholm, S-104 05 Stockholm, Sweden

(*Received* 21 *November* 1974; *accepted* 22 *January* 1975)

The structure of Mo_5O_{14} was solved previously in projection and found to be a 'tunnel structure', similar to those of $Mo_{17}O_{47}$ and $W_{18}O_{49}$, consisting of MoO_6 octahedra and MoO_7 pentagonal bipyramids. Crystals of this phase, stabilized by substitution of tantalum for 7% of the molybdenum, have been studied by single-crystal diffractometry. A refinement of the (seemingly) tetragonal projection ($a'' \simeq 23$ Å) indicates that tantalum substitutes exclusively in the pentagonal bipyramids. Like the binary phase, these crystals exhibit a superstructure and concomitant twinning associated with off-centre displacements of the atoms (puckering) along the short c ($\simeq 4$ Å) axis. From an observed slight difference in the relative amounts of the two twin components in one crystal, it could be concluded that the symmetry of the superlattice is orthorhombic, with $a = 2a''$ and $b = a''$, and not tetragonal as suggested previously. The puckering scheme and the three-dimensional structure were determined by the use of partial Patterson functions calculated from the twin-free superlattice reflexions. The twinning and disorder are readily understood as results of the pronounced pseudosymmetry. The degree of twinning and the size of the coherently scattering regions seem related to the conditions of formation.

Introduction

In a study of the molybdenum–oxygen system a phase called θ-oxide was observed to form in a very narrow temperature interval around 500°C (Kihlborg, 1959). It was assumed to be metastable at the formation temperature since it appeared only in samples heat-treated for short periods of time and decomposed upon prolonged heating. Single-crystal studies revealed an apparently tetragonal lattice with the axes $a'' \simeq 23$ Å and $c \simeq 4$ Å, but diffuse spots in the upper layers ($l > 0$) implied a superlattice with $a' \simeq 46$ Å. The substructure, solved in projection along **c**, indicated the formula Mo_5O_{14}, in good agreement with the phase analysis. The essential problem left unsolved was to determine the signs of the displacements $\pm \Delta z$, of metal atoms from a common plane perpendicular to **c**, which give rise to the superstructure. The diffuseness of the superlattice reflexions and conflicting symmetry conditions indicated disorder and twinning associated with this superstructure (Kihlborg, 1963*a*).

It was later observed that a substitution of some transition metals for part of the molybdenum stabilizes this phase (Kihlborg, 1969). Extensive phase studies have demonstrated this effect with vanadium (Ekström & Nygren, 1972*a*), niobium, tantalum (Ekström & Nygren, 1972*b*) and titanium (Ekström, 1972) as substituting elements.

In these ternary systems the M_5O_{14} phase formed quite reproducibly and at temperatures high enough for the growth of single crystals. This made possible the renewed investigation of the M_5O_{14} structure presented below.

Tantalum was chosen as the substituent in this study for two reasons. First, tantalum has a scattering power substantially different from that of molybdenum so that ordering on specific sites should be clearly revealed. Second, the likelihood of getting single crystals of sufficient size seemed greatest in this case since the tantalum phase is stable up to its melting point ($\simeq 848$ °C), as reported by Ekström & Nygren (1972*b*). The tantalum content x in $(Ta_xMo_{1-x})_5O_{14}$ was found to have a maximum range of $0{\cdot}06 < x < 0{\cdot}08$ and the unit-cell dimensions were $a'' = 22{\cdot}88 \pm 0{\cdot}005$ Å and $c = 4{\cdot}003 \pm 0{\cdot}002$ Å (from the powder pattern where no superlattice reflexions can be seen) with no significant variations observed (Ekström & Nygren, 1972*b*).

A structural complication has been discovered by electron diffraction. The binary Mo_5O_{14}, as well as all partly substituted phases including the tantalum compound, invariably show weak extra spots in the electron diffraction patterns, necessitating a doubling also of the c axis. Their presence, irrespective of beam intensity and crystal thickness, makes it unlikely that they result from structural changes caused by beam heating in the electron microscope. These reflexions were then also seen as extremely weak spots on heavily exposed X-ray rotation photographs. The origin of this additional superstructure is not known but the weakness of the X-ray reflexions indicates that it must be a very subtle structural modification. This doubling of the c axis is disregarded in the following and l and z (without primes) will refer to the short c' axis.

Synthesis and data collection

The starting materials were tantalum pentoxide (Koch-Light Lab., 99·9%), molybdenum trioxide (Mallinckrodt, Anal. Reag.) and molybdenum dioxide (prepared

* On leave from Department of Applied Chemistry, Kyushu University, Fukuoka, Japan.

from MoO_3 by reduction with a H_2/H_2O mixture). A weighed mixture of composition $Mo_{0.93}Ta_{0.07}O_{2.80}$ was sealed in an evacuated silica tube, heated to above 850°C, then cooled at a rate of 1·5°C h^{-1} to 770°C and from then rapidly to room temperature.

Microscopic observations indicated the sample to be a single phase consisting of brownish-yellow needle-shaped crystals, most of which aggregated into bundles. The X-ray powder pattern recorded with a Guinier–Hägg focusing camera displayed no impurity lines. The lattice parameters (Table 1) are in good agreement with the values reported for $(Mo_{0.93}Ta_{0.07})_5O_{14}$.

Table 1. *Lattice dimensions*

Subcell (tetragonal)

$(Mo_{0.93}Ta_{0.07})_5O_{14}$	Mo_5O_{14}
$a''=22{\cdot}873$ (2) Å	$a''=23{\cdot}00$ Å
$c' = 4{\cdot}0023$ (6)	$c' = 3{\cdot}937$

Apparent supercell (tetragonal)

$$a'=2a'' \qquad c'=c'$$

True supercell (orthorhombic)

$$a=2a'' \qquad b=a'' \qquad c=2c'^{*}$$

* This doubling is not accounted for in the present investigation; see *Introduction*.

X-ray diffraction data were collected from two crystals of different size with different instruments and different radiation, as indicated in Table 2. Difficulties in resolving reflexions were encountered with data set I, collected with Mo radiation. A narrow receiver aperture (semiangle 0·0047 rad) improved peak separations. Despite this, high-index reflexions in some regions had to be excluded because of unsatisfactory resolution. Cu radiation was used for data set II and a smaller crystal was chosen to reduce absorption. Although this data set is less accurate than data set I because of shorter time allowed for the measurements, the smaller crystal size turned out to be advantageous in the treatment of the twinning problem, as discussed later.

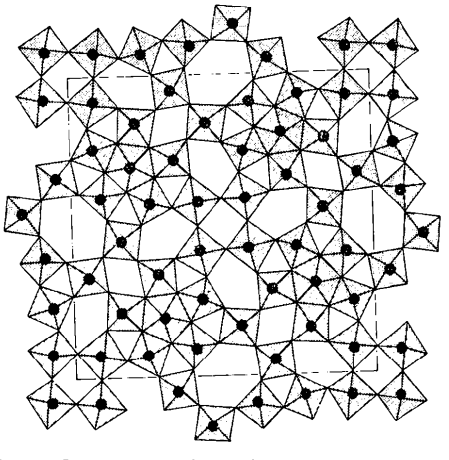

Fig. 1. The M_5O_{14} structure in projection along [001], depicted as linked MO_6 octahedra and MO_7 pentagonal bipyramids. The extent of the tetragonal subcell is outlined.

Table 2. *Summary of data collection*

Indices are based on the apparent (tetragonal) supercell.

Data set	I	II
Radiation	Mo $K\alpha$	Cu $K\alpha$
Diffractometer	Siemens AED (double scan)	Philips PW 1100 (single scan)
Crystal	{110} prism	{110} prism
size (mm)	0·05 × 0·04 × 0·15	0·025 × 0·02 × 0·15
Twin ratio	51:49	60:40
Number of reflexions collected;		
[$\sigma(I)/I \le 0.50$, within one octant]		
h' even, k' even, $l=0$	770	468
h' even, k' even, $l\ge 1$	749	588
h' odd, k' even, $l\ge 1$	661	489
h' even, k' odd, $l\ge 1$	673	436

The data were corrected for absorption. The atomic scattering factors of Mo, Ta and O were taken from Cromer & Waber (1965) and the anomalous dispersion factors for Mo and Ta were those of Cromer (1965). Full-matrix least-squares refinement was performed with the parameter in Hughes's weighting scheme* adjusted to give a satisfactory weight analysis.

Structure determination

The Mo_5O_{14} structure previously determined in projection is depicted in Fig. 1 as a network of MoO_6 octahedra and MoO_7 pentagonal bipyramids. Along the short projection axis the polyhedra are simply stacked on top of one another, sharing corners. By analogy with other similar oxides the oxygen atoms were supposed to be situated close to $z=0$ or $z=\frac{1}{2}$ and the metal atoms close to $z=0{\cdot}425$ or $z=0{\cdot}575$. The latter was supported by the intensity distribution among the $00l$ reflexions. The symmetry of the projection was found to be $p4g$; at least, no deviation from this symmetry could be detected.

As mentioned briefly above, diffuse extra reflexions in the upper layers ($l>0$) implied a superlattice with $a'=2a''\simeq 46$ Å and the apparent Laue symmetry $4/mmm$ retained. In this tetragonal superlattice the following systematic absences were found:

(1) $h'k'l$ for h' and k' both odd
(2) $h'k'0$ for either h' or k' odd
(3) $h'00$ for $h'\neq 4n$.

Condition (1) is not required by any space group, but it was shown that space group $P4/n$ combined with the substructure would give rise to this condition. No solution of the three-dimensional structure could be found, however.

The rotation and Weissenberg patterns of the $(Ta,Mo)_5O_{14}$ crystals were very similar to those of

* Weight $w=1/F_o^2$ for $F_o > C$ and $w=1/C^2$ for $F_o \le C$, where C is a constant.

Mo_5O_{14} from the previous investigation but the superlattice reflexions were sharper, in fact only slightly more diffuse than the sublattice spots.

The structure analysis commenced with a refinement of the *hk*0 projection and included a determination of the tantalum distribution. Then three-dimensional analysis was undertaken.

Refinement of the [001] projection

The projection of the structure along [001] was refined using the *x* and *y* coordinates from Mo_5O_{14} as starting parameters. The symmetry was assumed to be *p*4*g* and 770 subcell reflexions *h''k''*0 of data set I were used.

With equal scattering factors for all metal sites the discrepancy index $R=\sum|F_o-F_c|/\sum|F_o|$ did not drop below 0·20. This suggested that the distribution of the tantalum atoms was not random but ordered. A very reasonable structure was then an arrangement with tantalum in the pentagonal bipyramids and molybdenum in all octahedra. With a tantalum content of 7 at.% the statistical composition Ta/Mo on sites M(1) within the pentagonal bipyramids would be 7/3, and a corresponding compound scattering factor was used. This model quickly refined to $R=0{\cdot}022$ and an occupancy parameter introduced for M(1) did not deviate significantly from unity.

The oxygen atoms O(1) to O(6) are superimposed on the corresponding metal atoms in this projection and the temperature factors of these oxygens were too strongly correlated with those of the metals to permit their refinement. The *B* values for these oxygen atoms were therefore kept fixed at 0·80 Å^2. The resulting parameters are given in Table 3.

Table 3. *Parameters obtained from refinement in projection*

Space group: *p*4*g*
Subcell dimensions: $a''=22{\cdot}873$ Å ($c'=4{\cdot}0023$ Å)
Subcell content: 8 $(Mo_{0\cdot93}Ta_{0\cdot07})_5O_{14}$
M = (0·3 Mo + 0·7 Ta), resulting occupancy factor 2 × 0·4976 (16)

	Position	$x''(\sigma)$	$y''(\sigma)$	$B(\sigma)$ Å^2
M(1)	4(*c*)	0·29954 (8)	$\frac{1}{2}-x$	0·34 (1)
Mo(2)	4(*c*)	0·40284 (7)	$\frac{1}{2}-x$	0·35 (2)
Mo(3)	8(*d*)	0·04899 (6)	0·33865 (5)	0·42 (2)
Mo(4)	8(*d*)	0·08336 (4)	0·07612 (4)	0·51 (2)
Mo(5)	8(*d*)	0·15835 (7)	0·21907 (8)	0·28 (1)
Mo(6)	8(*d*)	0·24011 (4)	0·07321 (4)	0·52 (2)
O(1)	4(*c*)	0·3017 (14)	$\frac{1}{2}-x$	(0·80)
O(2)	4(*c*)	0·3980 (8)	$\frac{1}{2}-x$	(0·80)
O(3)	8(*d*)	0·0501 (5)	0·3441 (5)	(0·80)
O(4)	8(*d*)	0·0899 (4)	0·0814 (4)	(0·80)
O(5)	8(*d*)	0·1609 (7)	0·2203 (7)	(0·80)
O(6)	8(*d*)	0·2487 (4)	0·0715 (4)	(0·80)
O(7)	4(*c*)	0·0997 (4)	$\frac{1}{2}-x$	0·44 (11)
O(8)	4(*c*)	0·2354 (4)	$\frac{1}{2}-x$	0·52 (11)
O(9)	8(*d*)	0·2730 (2)	0·0033 (2)	0·57 (8)
O(10)	8(*d*)	0·0050 (2)	0·0818 (2)	0·76 (9)
O(11)	8(*d*)	0·1054 (2)	0·1597 (2)	0·69 (9)
O(12)	8(*d*)	0·1124 (2)	0·2825 (2)	0·59 (9)
O(13)	8(*d*)	0·1663 (2)	0·0601 (2)	0·52 (8)
O(14)	8(*d*)	0·2229 (2)	0·1594 (2)	0·46 (8)
O(15)	8(*d*)	0·3159 (2)	0·1126 (2)	0·48 (8)
O(16)	8(*d*)	0·3898 (2)	0·0203 (2)	0·68 (9)

Analysis of the three-dimensional structure

The main features of the structure are given by the projection, since all polyhedra must be at the same level, with the oxygens located close to $z=0$ or $\frac{1}{2}$ and the metal atoms around $z\simeq\frac{1}{2}$. As mentioned above, it was already clear from the previous investigation that the extension from the substructure to the superstructure is associated with a displacement of the metal atoms by + or $-\Delta z$ from the plane $z=\frac{1}{2}$. The substructure can thus be regarded as the limiting case of complete disorder, *i.e.* an average structure in which the metal atoms occupy the two possible positions with equal statistical weights. This model was supported by a calculation of structure factors for the subcell reflexions with $l\geq1$ (data set I), with the parameters of Table 3, and the *z* coordinates for the metal atoms (occupancy = $\frac{1}{2}$) taken to be $\frac{1}{2}\pm0{\cdot}075$. The *R* value for this calculation was 0·12.

In the actual structure the metal atoms occupy one of the two possible positions. The structure can thus be represented by a sum of two electron density functions: one corresponding to the average structure and the other to the deviation from this. The latter function is positive at the occupied positions and negative at the alternative unoccupied sites. The autoconvolution of the 'deviation function' is the partial Patterson function, calculated from the superlattice reflexions alone (Buerger, 1956). An analysis of the relationship between the appearance of the partial Patterson functions and the deviation structure was recently given by Takeuchi (1972).

The present case is particularly simple since the pairs of alternative positions are all lined up parallel to [001] and have the same separation of $2\Delta z$, at least approximately. Therefore, the resulting inter-

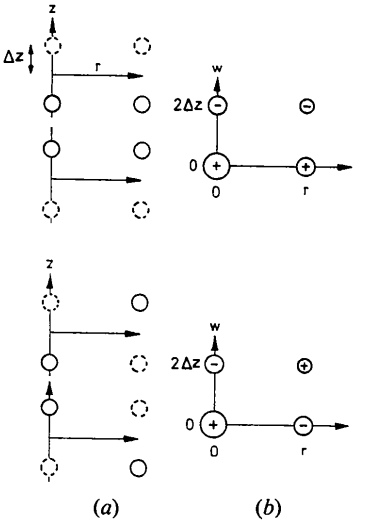

Fig. 2. Pairs of atoms (*a*) and corresponding partial Patterson functions (*b*). Non-occupied positions indicated by broken circles.

atomic vectors in the partial Patterson map will appear in the sections $w=0$ and $w=2\Delta z$ as peaks of positive or negative sign depending on the mutual relation between the shifts of the two atoms, as indicated in Fig. 2.

The partial Patterson map calculated on the basis of the apparent tetragonal supercell with $a'=45{\cdot}75$ Å and $c'=4{\cdot}002$ Å gave no satisfactory structure model. A careful analysis of data set II revealed that the intensities of the superstructure reflexions $h'0l$ and $0k'l$ differ significantly, in contradiction to tetragonal symmetry. The following general intensity relations were observed

(1) $I(h'k'l)\simeq I(k'h'l)$ for h' and k' even simultaneously
(2) $I(h'k'l)=I(k'h'l)=0$ for h' and k' odd simultaneously
(3) $I(h'k'l)\,/\,I(k'h'l)\simeq 0{\cdot}66$ for h' even and k' odd
(4) $I(h'k'l)\,/\,I(k'h'l)\simeq 1{\cdot}52$ for h' odd and k' even.

Relation (2) is the apparent extinction condition mentioned earlier. The maximum deviations from the mean values of the ratios given in (3) and (4) were $\pm 0{\cdot}16$.

These relations can be explained by assuming twinning across {210} in an *orthorhombic* lattice with $a=a'$ and $b=\frac{1}{2}a'=a''$ and a twin ratio of 0·66 or $\frac{40}{60}$. A similar inspection of data set I gave a twin ratio of $\frac{49}{51}$. It can be seen from Fig. 3 that with this lattice the subcell reflexions are always a mixture of hkl and $2k,\frac{1}{2}h,l$ from the two individuals, while the superlattice reflexions are pure.

Partial Patterson maps were now calculated on the basis of the orthorhombic lattice from the superlattice reflexions of the dominating twin (Fig. 4). It was now possible to derive a structure model (Fig. 5) consistent with the partial Patterson function. This model gives rise to a very large number of interpair vectors but the majority of these vanish because they are superimposed on other vectors of opposite sign. Non-vanishing vectors are shown in Fig. 4 together with a partial Patterson map.

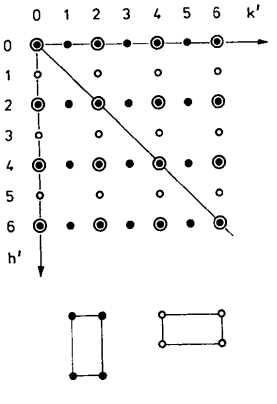

Fig. 3. Reciprocal-lattice plane ($l\neq 0$) resulting from superposition of the two orthorhombic twin cells shown below. Indices refer to the seemingly tetragonal supercell.

The space group of this structure is $Pb2_1a$ [No. 29 in *International Tables for X-ray Crystallography* (1952) in a non-conventional setting and with origin shifted to bring it into concordance with the substructure].

In the first refinement of this model only the metal atoms were included and their x and y coordinates were kept fixed at the values given in Table 3 (with the different unit-cell taken into account). With the temperature factors also held constant (at $B=0{\cdot}50$ Å^2) a refinement *versus* 661 supercell reflexions (h odd) from data set I gave reasonable z values, ranging from $\pm 0{\cdot}395$ to $\pm 0{\cdot}435$, and a discrepancy index $R=0{\cdot}06$. A similar refinement *versus* 489 reflexions from data set II gave $R=0{\cdot}08$.

However, when the temperature factors were refined they became negative for all (data set I) or some (data set II) of the atoms. In addition, the scale factors were significantly less than expected on the basis of the previous substructure refinement, about 30% less for data set I and about 5% for data set II. This indicated that approximately 50% and 10%, respectively, of the intensity was systematically missing for the superstructure reflexions.

This phenomenon arises from use of too narrow X-ray detector apertures. To improve resolution, the narrowest receiving slits which did not affect the integrated intensities of the strong subcell test reflexions were used. The supercell reflexions were slightly broader, however, and the slit apertures were obviously too small for these. It can be shown* that this leads to a larger intensity loss at low θ angles than at high, which thus explains the negative temperature factors for the superstructure reflexions.

The differences between the results obtained from data set I and data set II may be due to the differences in crystal size, radiation, diffractometer, apertures *etc.*

In the subsequent refinement the 661 superstructure reflexions of data set I were grouped into five $\sin\theta$ intervals with a variable scale factor for each group. Only z, the scale factor, and a group temperature factor common to all metal atoms were refined; the temperature factors for all oxygen atoms were fixed at 0·40 Å^2. The R value decreased to 0·037. No further refinement was made *versus* data set II, which was of lower accuracy.

Full three-dimensional refinement *versus* the superstructure reflexions was not attempted since the ratio between the number of observations and the number of parameters was considered too low. The substruc-

* Assume the intensity distribution in the reciprocal lattice to be Gaussian with spherical symmetry, approximated by

$$I(w)=J_0\sigma/\{\sigma^2+(\pi w)^2\}$$

where w is the distance from the reciprocal-lattice point and J_0 and σ are constants related with the peak height and width, respectively. Then the ratio between the intensity I, obtained from a θ–2θ scan with too narrow a receiver aperture of divergence angle D, and the total intensity I_0 can be approximated by the equation $I/I_0\simeq k_1\,.\,\arctan\{k_2\,.\,D\,.\,(\sin\theta/\lambda)\}$, where k_1 and k_2 are constants.

Table 4. *Three-dimensional structure*

x and y parameters from refinement in projection (Table 3).
Space group: $Pb2_1a$ (No. 29).
Unit cell: $a=45{\cdot}75$ Å, $b=22{\cdot}87$ Å, $c'=4{\cdot}0023$ Å.
Atom designation: The number following the letter symbol is consistent with the number in the subcell (Table 3). The succeeding letters serve to distinguish between atoms which are symmetry-related in the subcell, according to the following scheme:

AA	x'',y''	*BB*	$\frac{1}{2}+x'',\frac{1}{2}-y''$
AB	$\frac{1}{2}-y'',\frac{1}{2}-x''$	*A*	$x'',\frac{1}{2}-x''$
BA	$\bar{y}'',x''$	*B*	$\frac{1}{2}+x'',x''$

	Atom	x (σ)	y (σ)	z (σ)
1	M 1A	0.14976(4)	0.20046(8)	0.4350(8)
2	M 2A	0.20142(3)	0.09715(7)	0.5805(16)
3	M 3AA	0.02449(3)	0.33864(5)	0.4025(16)
4	M 4AA	0.04167(2)	0.07611(4)	0.4207(16)
5	M 5AA	0.07917(4)	0.21906(8)	0.5852(18)
6	M 6AA	0.12005(2)	0.07321(4)	0.6007(16)
7	M 3AB	0.08067(2)	0.45101(5)	0.5873(17)
8	M 4AB	0.21194(2)	0.41664(4)	0.4170(17)
9	M 5AB	0.14046(4)	0.34165(7)	0.5852(16)
10	M 6AB	0.21339(2)	0.25988(3)	0.6012(16)
11	M 1B	0.39976(4)	0.29953(8)	0.5729(9)
12	M 2B	0.45142(3)	0.40284(7)	0.4272(15)
13	M 3BA	0.33067(2)	0.04898(5)	0.5940(18)
14	M 4BA	0.46194(2)	0.08335(4)	0.4196(17)
15	M 5BA	0.39046(4)	0.15834(7)	0.4179(17)
16	M 6BA	0.46339(2)	0.24011(3)	0.4161(17)
17	M 3BB	0.27449(3)	0.16135(5)	0.4123(16)
18	M 4BB	0.29167(2)	0.42388(4)	0.5797(16)
19	M 5BB	0.32917(4)	0.28093(8)	0.4151(18)
20	M 6BB	0.37005(2)	0.42678(4)	0.4049(15)
21	O 1A	0.15084(68)	0.19830(136)	0.9828(58)
22	O 2A	0.19898(39)	0.10202(78)	0.0118(55)
23	O 3AA	0.02504(24)	0.34410(47)	0.9844(58)
24	O 4AA	0.04493(19)	0.08140(37)	0.9967(54)
25	O 5AA	0.08043(34)	0.22032(72)	0.9942(59)
26	O 6AA	0.12435(18)	0.07150(35)	0.0137(62)
27	O 3AB	0.07794(23)	0.44990(49)	0.0066(56)
28	O 4AB	0.20929(19)	0.41012(37)	0.0016(56)
29	O 5AB	0.13983(36)	0.33912(68)	0.0100(56)
30	O 6AB	0.21424(18)	0.25130(36)	0.0202(61)
31	O 1B	0.40084(68)	0.30169(136)	0.0159(59)
32	O 2B	0.44898(39)	0.39797(78)	0.0069(56)
33	O 3BA	0.32794(23)	0.05009(49)	0.0124(61)
34	O 4BA	0.45929(19)	0.08987(37)	0.9938(59)
35	O 5BA	0.38983(36)	0.16087(68)	0.9954(58)
36	O 6BA	0.46424(18)	0.24869(36)	0.9912(58)
37	O 3BB	0.27504(24)	0.15589(47)	0.9895(57)
38	O 4BB	0.29493(19)	0.41859(37)	0.0018(54)
39	O 5BB	0.33043(34)	0.27967(72)	0.9953(62)
40	O 6BB	0.37435(18)	0.42849(35)	0.9817(54)
41	O 7A	0.04986(20)	0.40026(40)	0.4936(59)
42	O 8A	0.11770(20)	0.26458(39)	0.4913(61)
43	O 9AA	0.13647(10)	0.00336(20)	0.5254(68)
44	O10AA	0.00251(11)	0.08179(21)	0.5076(58)
45	O11AA	0.05268(11)	0.15968(21)	0.4973(59)
46	O12AA	0.05621(10)	0.28251(20)	0.4885(65)
47	O13AA	0.08315(10)	0.06009(20)	0.5098(58)
48	O14AA	0.11143(10)	0.15938(19)	0.5068(55)
49	O15AA	0.15795(10)	0.11260(20)	0.5093(59)
50	O16AA	0.19491(11)	0.02029(22)	0.4942(60)
51	O 9AB	0.24831(10)	0.22704(20)	0.5107(61)
52	O10AB	0.20910(11)	0.49497(21)	0.5157(65)
53	O11AB	0.17016(10)	0.39464(21)	0.5098(60)
54	O12AB	0.10874(10)	0.38756(20)	0.5128(58)
55	O13AB	0.21995(10)	0.33369(20)	0.5120(57)
56	O14AB	0.17030(10)	0.27712(20)	0.5050(63)
57	O15AB	0.19369(10)	0.18409(20)	0.5054(57)
58	O16AB	0.23985(11)	0.11016(21)	0.5035(58)
59	O 7B	0.29986(20)	0.09973(40)	0.5156(66)
60	O 8B	0.36770(20)	0.23541(39)	0.5036(57)
61	O 9BA	0.49831(10)	0.27295(20)	0.4801(66)
62	O10BA	0.45910(11)	0.00502(21)	0.4987(60)
63	O11BA	0.42016(10)	0.10535(21)	0.4860(63)
64	O12BA	0.35874(10)	0.11243(20)	0.5141(61)
65	O13BA	0.46995(10)	0.16630(20)	0.4950(56)
66	O14BA	0.42030(10)	0.22287(20)	0.5014(61)
67	O15BA	0.44369(10)	0.31590(20)	0.5089(57)
68	O16BA	0.48985(11)	0.38983(21)	0.5290(64)
69	O 9BB	0.38647(10)	0.49663(20)	0.4907(61)
70	O10BB	0.25251(11)	0.41820(21)	0.4896(56)
71	O11BB	0.30268(11)	0.34031(21)	0.4852(58)
72	O12BB	0.30621(10)	0.21748(20)	0.4998(58)
73	O13BB	0.33315(10)	0.43990(20)	0.4950(58)
74	O14BB	0.36143(10)	0.34061(19)	0.4881(59)
75	O15BB	0.40795(10)	0.38739(20)	0.5118(59)
76	O16BB	0.44491(11)	0.47970(22)	0.5093(59)

ture reflexions were of little value for such a refinement because they were affected by twinning. The final parameters given in Table 4 have therefore been obtained from the one- and two-dimensional refinements. The x and y coordinates resulted from the two-dimensional substructure refinement and have simply been re-ex-

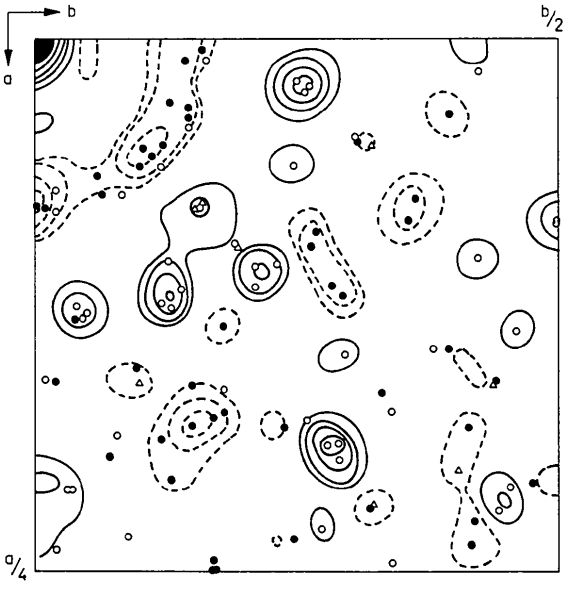

Fig. 4. Partial Patterson section at $w=0$ with non-vanishing vectors obtained from the model of Fig. 5. Open circles = positive vectors, filled circles = negative vectors. Triangles have half weight.

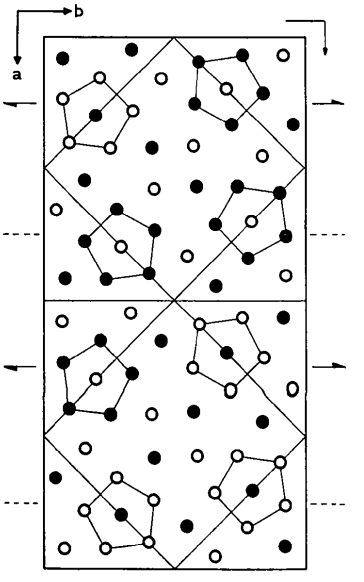

Fig. 5. Metal-atom positions in the orthorhombic unit-cell with displacements up (= open circles) or down (= filled circles) from the plane $z=\frac{1}{2}$ indicated. The peripheral metal atoms in the pentagonal columns have been connected by lines for sake of clarity and the (apparent) diagonal mirror lines of the projection are also indicated.

pressed in terms of the different unit-cell. The *hk*0 zone contained no superstructure reflexions and the quality of the data seemed rather good, to judge from the low R value ($R=0{\cdot}022$). The reasonable temperature factors and low standard errors obtained indicate that the deviation from the assumed tetragonality in this projection must be very small. The z values of Table 4 are from the above-mentioned superstructure refinement with the x and y coordinates fixed.

The parameters of Table 4 give an R value of 0·040 when calculated for all observed data. It is obvious, however, that the model thus derived and refined is only an approximation. Deviations, however small, from the tetragonality in projection must be present. It should also be remembered that the doubling of the c axis revealed by electron diffraction (see above) has not been taken into account.

Discussion

A description of the structure in terms of linked polyhedra has been given previously (Kihlborg, 1963*a*) and most features are evident in Fig. 1. The additional information obtained from the present study concerns the mechanism of metal atom substitution and the pattern of puckering of the metal atoms.

It has been demonstrated in the present study that tantalum substitutes exclusively in the pentagonal bipyramids. This is not unexpected in view of the frequent occurrence of tantalum in seven-coordination with oxygen (see for example a review by Jahnberg, 1971). Tantalum thus behaves differently from vanadium in the $M_{17}O_{47}$ structure which also contains 'pentagonal columns' (a pentagonal bipyramid surrounded by five octahedra). There, vanadium prefers two octahedral sites near a metal–metal bond (Yamazoe, Ekström & Kihlborg, 1975). Though atomic size may play an important role here the reduction in the number of nonbonding valence electrons upon substitution is probably responsible for the increased stability of the substituted phases (Ekström, 1972*b*). It would be interesting to learn how vanadium is distributed in the M_5O_{14} structure, but suitable single crystals have not yet been obtained.

The puckering of the metal-atom layers is a significant feature in this structure. The average displacement from the plane $z=\frac{1}{2}$ is 0·348 Å. Since the oxygen atoms remain close to $z=0$ this gives rise to one short and one long M–O bond. For the octahedra the short distances range from 1·64 (3) to 1·73 (2) Å and the long from 2·37 (2) to 2·28 (2) Å, with an average difference of 0·632 Å. The corresponding distances in the two pentagonal bipyramids are 1·77 (2), 1·81 (2), 2·23 (2) and 2·19 (2) Å with an average difference of 0·434 Å. The metal atoms M(1) within the pentagonal bipyramids, which are 70% Ta, are thus on the whole less displaced than the molybdenum atoms in the octahedra. The equatorial M–O bonds (those approximately in the xy plane) range from 1·74 (1) to 2·08 (1) Å, average 1·899 Å, in the octahedra and from 2·01 (1) to 2·09 (1) Å, average 2·047 Å, in the pentagonal bipyramids.

Off-centre displacement of metal atoms is frequently encountered in transition-metal oxides and is found in all molybdenum oxides. The predominant type in many of these is a one-dimensional puckering similar to that found in the present structure. The puckering amplitude is correlated with the average valence of the molybdenum, as seen from Table 5 in which V and Ta are assumed pentavalent. This is only a rough scheme, however, since the detailed distortion pattern for individual metal atoms may be rather different in these oxides (Kihlborg, 1963*b*).

Table 5. *Puckering amplitudes*

Compound	Average valence of Mo	Average displacement from a common plane
$Mo_{17}O_{47}$	5·53	0·298 Å
$(Mo_{0\cdot93}V_{0\cdot07})_{17}O_{47}$	5·57	0·330
$(Mo_{0\cdot93}Ta_{0\cdot07})_5O_{14}$	5·65	0·348
Mo_8O_{23}	5·75	0·356
MoO_3	6·00	0·415*

* Displacement resulting from components along two perpendicular directions.

From a simple electrostatic point of view one would expect neighbouring metal atoms to be oppositely displaced. This is obviously not everywhere possible in the present structure, which contains many rings of an odd number of octahedra. It is, however, the dominant type of displacement between close pairs, as is evident from the negative region closest to the origin in the partial Patterson section at $w=0$ (Fig. 4). Only in 16 of the total of 96 pairs are the atoms at the same level, not counting the intermetal vectors within the pentagonal columns.

The displacements of the central metal atoms in the pentagonal columns are opposite to those in the surrounding five octahedra. This is reasonable since the metal–metal separations from the central atom (across the shared edges) are considerably shorter ($\simeq 3{\cdot}33$ Å) than the peripherial ones ($\simeq 3{\cdot}86$ Å).

The corresponding configuration in $Mo_{17}O_{47}$ is somewhat different. There the metal in one of the octahedra surrounding the pentagonal bipyramid is displaced in *the same* direction as the central atom. The surroundings of the pentagonal columns are, however, rather different in the two structures and this particular octahedron in $Mo_{17}O_{47}$ has a rather unique structural role.

Although the four-rings of octahedra in the middle and corners of the subunits (around $x,y=0,0$; $\frac{1}{4},\frac{1}{2}$; $\frac{1}{2},0$ in Fig. 5) as well as the six-rings (around $0,\frac{1}{2}$; $\frac{1}{4},0$; $\frac{1}{2},\frac{1}{2}$) have the expected staggered configuration, the four-rings surrounding the pentagonal bipyramids cannot, because the two octahedra belonging to the pentagonal columns are both either up or down. These four-rings have instead a 3–1 configuration.

The three-rings are the most interesting ones. Most of these have the expected 2–1 configuration, but one of eight has all three metals displaced in the same direction. If this one were the same as the others, the two halves of the asymmetric unit would have the same type of puckering and be related by a twofold screw axis parallel to **a**. This could increase the symmetry but would then give rise, for instance, to four-rings of the type $++++$ and six-rings with $+--+--$ configuration. It would require a thorough topological investigation to find whether the present puckering pattern gives rise to the highest possible number of opposite neighbours.

It is quite obvious that twinning is very likely to occur in a structure of this kind. With the pseudosymmetry described above, it requires very few mistakes in the puckering for the *a* and *b* axes to become interchanged. The degree of twinning and the size of the coherently scattering regions seem related to the conditions of formation. The crystals of binary Mo_5O_{14}, which gave very diffuse superlattice reflexions, had been prepared by relatively short ($\sim$1 d) heat treatment at low temperature (520°C) and were evidently much more densely twinned than the crystals studied here, which grew very slowly from the melt. Schröder (1972) reported that Mo_5O_{14} crystals prepared by reducing MoO_3 in a stream of HCl gas gave no superstructure reflexions at all. Considering that the crystal growth was very rapid in that case (completed in the order of 10 min) it seems likely that the coherent regions were so small that the superstructure spots completely disappeared in the background.

This investigation forms part of a research program supported by the Swedish Natural Science Research Council. N.Y. acknowledges a scholarship from the Japan–Sweden Foundation, Tokyo.

References

BUERGER, M. J. (1956). *Proc. Nat. Acad. Sci.* **42**, 776.
CROMER, D. T. (1965). *Acta Cryst.* **18**, 17–23.
CROMER, D. T. & WABER, J. T. (1965). *Acta Cryst.* **18**, 104–109.
EKSTRÖM, T. (1972*a*). *Acta Chem. Scand.* **26**, 1843–1846.
EKSTRÖM, T. (1972*b*). *Mater. Res. Bull.* **7**, 19–26.
EKSTRÖM, T. & NYGREN, M. (1972*a*). *Acta Chem. Scand.* **26**, 1827–1835.
EKSTRÖM, T. & NYGREN, M. (1972*b*). *Acta Chem. Scand.* **26**, 1836–1842.
International Tables for X-ray Crystallography (1952). Vol. I. Birmingham: Kynoch Press.
JAHNBERG, L. (1971). *Chem. Commun. Univ. Stockholm*, No. XIII.
KIHLBORG, L. (1959). *Acta Chem. Scand.* **13**, 954–962.
KIHLBORG, L. (1963*a*). *Ark. Kem.* **21**, 427–437.
KIHLBORG, L. (1963*b*). *Ark. Kem.* **21**, 471–495.
KIHLBORG, L. (1969). *Acta Chem. Scand.* **23**, 1834.
SCHRÖDER, F. A. (1972). *Z. Naturforsch.* **27***b*, 498–500.
TAKEUCHI, Y. (1972). *Z. Kristallogr.* **135**, 120–136.
YAMAZOE, N., EKSTRÖM, T. & KIHLBORG, L. (1975). *Acta Chem. Scand.* In the press.

Acta Cryst. (1975). B**31**, 1672

The Crystal and Molecular Structures of *cis*-Dichloroethylenediamineplatinum(II) *and* Palladium(II)

BY JOHN IBALL, MARY MACDOUGALL AND SHEELAGH SCRIMGEOUR
Chemistry Department, University of Dundee, Dundee, DD1 4HN, Scotland

(*Received* 13 *December* 1974; *accepted* 3 *February* 1975)

The structures of *cis*-M(en)Cl_2 (M = Pt, Pd) have been determined from diffractometer data and refined by least-squares calculations: $R = 0{\cdot}073$ for Pt(en)Cl_2 (437 reflexions) and 0·057 for Pd(en)Cl_2 (416 reflexions). The compounds are isomorphous, space group $C222_1$ with $Z = 4$. The metal atoms have a square-planar configuration and the ethylenediamine rings are puckered. Intermolecular Pt···Pt and Pd···Pd distances are 3·381 and 3·369 Å respectively.

Introduction

It has been shown that certain complexes of the Pt group metals exhibit interesting biological effects (Rosenberg, Van Camp & Krigas, 1965). At low concentrations some are effective bactericides while others stop cell division and force bacteria to grow into long filaments. Some of these complexes are also very potent broad-spectrum antitumour agents. Of the complexes tested on animals the following were the most potent: (1) *cis*-$Pt^{IV}(NH_3)_2Cl_4$, (2) *cis*-$Pt^{II}(NH_3)_2Cl_2$, (3) *cis*-$Pt^{II}enCl_2$, (4) *cis*-$Pt^{IV}enCl_4$. We report the structure of